

Molecular formations in ultracold mixtures of interacting and noninteracting atomic gases

T. Nishimura* and A. Matsumoto

*Department of Physics, Tokyo Metropolitan University,
1-1 Minami-Ohsawa, Hachioji, Tokyo 192-0397, Japan*

H. Yabu†

Department of Physics, Ritsumeikan University, Kusatsu, Shiga 525-8577, Japan

Abstract

Atom-molecule equilibrium for molecular formation processes is discussed for boson-fermion, fermion-fermion, and boson-boson mixtures of ultracold atomic gases in the framework of quasi-chemical equilibrium theory. After presentation of the general formulation, zero-temperature phase diagrams of the atom-molecule equilibrium states are calculated analytically; molecular, mixed, and dissociated phases are shown to appear for the change of the binding energy of the molecules. The temperature dependences of the atom or molecule densities are calculated numerically, and finite-temperature phase structures are obtained of the atom-molecule equilibrium in the mixtures. The transition temperatures of the atom or molecule Bose-Einstein condensations are also evaluated from these results. Quantum-statistical deviations of the law of mass action in atom-molecule equilibrium, which should be satisfied in mixtures of classical Maxwell-Boltzmann gases, are calculated, and the difference in the different types of quantum-statistical effects is clarified. Mean-field calculations with interparticle interactions (atom-atom, atom-molecule, and molecule-molecule) are formulated, where interaction effects are found to give the linear density-dependent term in the effective molecular binding energies. This method is applied to calculations of zero-temperature phase diagrams, where new phases with coexisting local-equilibrium states are shown to appear in the case of strongly repulsive interactions.

PACS numbers: 03.75.Mn, 05.30.-d, 31.15.bt, 82.60.Hc

* nimut@tmu.ac.jp

† yabu@se.ritsumei.ac.jp

I. INTRODUCTION

The experimental success of the Bose-Einstein condensation (BEC) [1] of the trapped ultracold atomic gas has made much progress in the physics of quantum gases[2, 3, 4], which includes Fermi-degenerate systems and Bose-Fermi mixtures.

Recently, using the Feshbach-resonance method, molecular formations have been performed experimentally in ultracold atomic gases for two fermions[5, 6, 8] and two bosons[7, 9]; Bose-Einstein condensations have been observed for the thus created molecules of two fermions[10, 11] and two bosons[9]. In these experiments, the molecular binding energies can be tuned by continuous changes of the applied magnetic fields; especially, bound molecular states can be changed into resonances by shifting the binding energies above the atom-atom scattering thresholds.

One of the interesting applications of ultracold molecules is the observation of the BEC-BCS crossover in experiments with atomic Fermi gases: continuous crossover between the strong-coupling molecular BEC and weak-coupling BCS superconducting states [12, 13, 14, 15, 16, 17]. In ultracold atomic-gas experiments, the crossover occurred by a change of the molecular binding energy through the Feshbach resonance method[18, 19, 20], and the experimental success has led to a lot of experimental and theoretical works on the crossover[21, 22, 23] and molecular BEC physics[24, 25].

Molecules in optical lattice potentials are also an interesting problem. After the first observation of molecular formations using ^{87}Rb [26], many experiments have been performed on the long-lived state of the ^{87}Rb molecule[27], ^{40}K difermion[28], and ^{87}Rb - ^{40}K boson-fermion heteronuclear molecules[29]. Quantum degeneracy has also been observed in gases of ^{87}Rb molecules[30]. The phase structure of the lattice-trapped atomic gas, which is produced through interparticle correlations, has much interest in relation to the strongly correlated condensed-matter system described by the Hubbard model. Thus many experimental and theoretical works have been done: for example, on the superfluid-Mott insulator transition in bosonic[31, 32, 33, 34, 35], fermionic [36, 37], and boson-fermion systems[38].

Other theoretical studies on ultracold molecules include coherent molecular solitons[39], coherent photoassociation[40], and coherent intercondensate exchange between atoms and molecules[41].

In this paper, we discuss atom-molecule equilibrium for boson-fermion, fermion-fermion,

and boson-boson mixtures of ultracold atomic gases with quasichemical equilibrium theory, an extension of classical chemical equilibrium theory[42, 43] for the quantum many-body problem, which was originally developed for the electron system in superconductors[12, 13]. Our special interest is in applications of this method to boson-fermion and boson-boson mixtures, especially occurrences of atom or molecule BEC, as shown in some works for boson-fermion mixtures[44, 45, 46, 47]. In addition, in contrast to the fermionic system, where many-body quantum calculations based on the microscopic model have been established, the singularities from the boson degrees of freedom sometimes cause problems in calculations of boson-fermion and boson-boson mixtures; quasichemical equilibrium theory can give definite solutions in such cases. As another interest of this approach, it should be pointed out that we can easily include interparticle interactions, especially atom-molecule and molecule-molecule ones, which are sometimes omitted in many-body calculations. The quasichemical approach gives the equilibrium structures in a less model-independent way. It turned out that the effects of these interactions should change the atom-molecule equilibrium structures drastically in the strong-coupling region.

In Sec. II, a general formulation of quasichemical equilibrium theory is presented for molecular formation or dissociation processes in noninteracting atomic-gas mixtures, and in Sec. III, the method is applied to boson-fermion, fermion-fermion, and boson-boson mixtures and the atom-molecule equilibrium structures are shown at zero and finite temperatures. Special attention is paid to the condition on the occurrences of atom or molecule BEC; the shifts of the BEC transition temperatures are discussed from the molecular binding energy effects. In Sec. IV, the law of mass action, which is satisfied in chemical processes with classical Boltzmann statistics, is shown to deviate in ultracold molecular formation or dissociation processes by quantum-statistical effects (the law of quantum mass action). In Sec. V, we extend the quasichemical theory to include interparticle interactions for *s*-wave scattering processes (three kinds of atom-atom ones, two kinds of atom-molecule ones, and one kind of molecule-molecule one in combination) in molecular formation or dissociation processes. In the mean-field approximation, the original six coupling constants of the interactions are shown to integrate into two parameters. It allows discussions of the interaction effects to be very clear. The formulations are applied to molecular formation or dissociation processes in interacting mixtures, and we discuss the change of the equilibrium structures at $T = 0$ through interaction effects; new phases with coexisting local-equilibrium states are shown

to appear in the case of strongly repulsive interactions. Section VI is devoted to a summary and outlook.

We should comment that a relativistic extension is also possible of quasichemical theory and applications to diquark condensates in quark matter have been done in [48].

II. QUASICHEMICAL EQUILIBRIUM THEORY ON MOLECULAR FORMATION IN ATOMIC-GAS MIXTURES

A. Molecular formation or dissociation process

Let us take an atomic-gas mixture consisting of two atomic species A_1 and A_2 with masses m_1 and m_2 ; in quantum statistics, $A_{1,2}$ are bosons or fermions, so that we have three kinds of combinations: boson-boson (BB), fermion-fermion (FF), and boson-fermion (BF).

To develop a quasichemical equilibrium theory, we consider a molecular formation or dissociation process in the mixture:

$$A_1 + A_2 \longleftrightarrow (A_1 A_2) = M, \quad (1)$$

where M is a composite molecule with mass m_M , which is bosonic in BB or FF mixtures and fermionic in BF mixtures.

The mass defect of the molecule is defined as $\Delta m_M \equiv (m_M - m_1 - m_2)$. The bound-molecule ($\Delta m_M < 0$) is stable in both vacuum and gases, and has molecular binding energy $\Delta E = \Delta m_M c^2$, where c is the velocity of light in vacuum. In contrast, the resonance ($\Delta m_M > 0$) is unstable at least in vacuum; however, resonance states can exist stably in gases, so that we consider both bound-molecule and resonance cases.

Here we take the quasiparticle picture wherein the system consists of atoms A_1 and A_2 and molecule M , which are quasiparticles[49]. In this picture, two-body interactions between “bare” atoms bring about two-body correlations in the mixture; their major effects are the creation of the composite molecule M with binding energy ΔE_M and atoms and molecules, which are quasiparticle in the mixture, and interact through residual interactions, which are generally different from the original interaction between bare atoms. These quasiparticle interactions are generally regarded to be weak, and we neglect them in the first part of this paper. In Sec. IV, we introduce the quasiparticle interactions and discuss their effects on atom-molecule equilibrium within the mean-field approximation.

The equilibrium condition for the process (1) is given by

$$\mu_1 + \mu_2 - \mu_M = \Delta E_M, \quad (2)$$

where $\mu_{1,2,M}$ are chemical potentials of A_1 , A_2 , and M .

The molecular binding energy ΔE_M in (2) is generally very small ($\sim 10^{-(5\sim 10)}$ eV) in molecular formation or dissociation processes in ultracold atomic-gases, and it takes the same order of magnitude with the chemical potentials of atoms or molecules μ_α at ultralow temperature ($T = \mu\text{K} - \text{nK}$). Thus, the term ΔE_M cannot be omitted in (2).

For free uniform gases, the particle densities are given by the Bose and Fermi statistics:

$$n_\alpha = \frac{1}{(2\pi)^3} \int \frac{d^3\mathbf{k}}{e^{(\varepsilon_\alpha - \mu_\alpha)/k_B T} - 1} + n_\alpha^{(0)} \equiv \frac{1}{(\lambda_{T,\alpha})^3} B_{3/2}(-\mu_\alpha/k_B T) + n_\alpha^{(0)} \text{ (for boson } A_\alpha), \quad (3)$$

$$n_\alpha = \frac{1}{(2\pi)^3} \int \frac{d^3\mathbf{k}}{e^{(\varepsilon_\alpha - \mu_\alpha)/k_B T} + 1} \equiv \frac{1}{(\lambda_{T,\alpha})^3} F_{3/2}(-\mu_\alpha/k_B T) \text{ (for fermion } A_\alpha), \quad (4)$$

where k_B is the Boltzmann constant and $\lambda_{T,\alpha}$ is the thermal de Broglie wave length of particle A_α at temperature T :

$$\lambda_{T,\alpha} = \sqrt{\frac{2\pi\hbar^2}{m_\alpha k_B T}}. \quad (5)$$

The one-particle energy ε_α in (3) and (4) is give by $\varepsilon_\alpha = \hbar^2 \mathbf{k}^2 / (2m_\alpha)$, where \mathbf{k} is the wave-number vector of particle A_α .

The B_A and F_A in (3) and (4) are the Bose and Fermi functions:

$$B_A(\nu) = \frac{1}{\Gamma(A)} \int_0^\infty \frac{x^{A-1} dx}{e^{x+\nu} - 1}, \quad (6)$$

$$F_A(\nu) = \frac{1}{\Gamma(A)} \int_0^\infty \frac{x^{A-1} dx}{e^{x+\nu} + 1}, \quad (7)$$

where ν corresponds to the fugacity and $\Gamma(A)$ is the gamma function. The Bose function B_A can be written with the Appel function $\phi(z, s)$ as $B_A(\nu) = \phi(A, e^\nu)$, and the Fermi function is expressed with the Bose functions $F_A(\nu) = B_A(\nu) - 2^{1-A} B_A(2\nu)$.

The Bose function B_A in (6) converges in $\nu \geq 0$ (or $\mu_\alpha \leq 0$ in the chemical potential) and becomes singular at $\mu_\alpha = 0$, with which a phase transition occurs to the Bose-Einstein condensate of the boson A_α . In the BEC region, the chemical potential vanishes and the condensed density $n_\alpha^{(0)}$ in (3) takes a finite value (it vanishes in the normal region).

In the process (1), the particle-number conservations for $A_{1,2}$ give the constraints

$$n_1 + n_M = n_{1,t}, \quad n_2 + n_M = n_{2,t}, \quad (8)$$

where $n_{1,t}$ and $n_{2,t}$ are the total number densities of atoms $A_{1,2}$, which consist of isolated atoms and constituents in the composite molecule M .

Solving Eqs. (2) and (8) with (3) and (4), we can determine the densities $n_{1,2,M}$ in equilibrium at temperature T for the parameters m_α , $n_{\alpha,t}$ ($\alpha = 1, 2$), and ΔE .

B. Scaled variables

We now introduce scaled dimensionless variables; they simplify the form of the above equations and greatly reduce the number of parameters.

The scaled masses \tilde{m}_α are defined by $\tilde{m}_\alpha = m_\alpha/m_M$, where $m_M = m_1 + m_2 + \Delta m_M$. In the ultracold atomic-gas system, the mass defect ($\Delta m_M \sim 10^{-5} - 10^{-10}$ eV) is highly smaller than the atom or molecule masses (\sim GeV); thus, we use the approximation $m_M \sim m_1 + m_2$ (the conservation law of mass in chemical processes) throughout this paper.

We introduce $n_t \equiv n_{1,t} + n_{2,t}$ and $E_s \equiv \hbar^2(n_t)^{2/3}/m_M$ as scaling quantities for the particle-number densities and the energies, respectively: for example, $\tilde{n}_\alpha = n_\alpha/n_t$ ($\alpha = 1, 2$, and M), $\tilde{T} = k_B T/E_s$, $\Delta\tilde{E}_M = \Delta E_M/E_s$, etc. E_s can be interpreted as having the meaning of the Fermi energy for the fermionic matter of fermions with mass m_M with density n_t , but we use it simply as a scaling quantity with the dimension of energy.

Using the scaled quantities, the equilibrium conditions (2) and (8) become

$$\tilde{\mu}_1 + \tilde{\mu}_2 - \tilde{\mu}_M = \Delta\tilde{E}_M, \quad (9)$$

$$\tilde{n}_1 + \tilde{n}_M = \tilde{n}_{1,t}, \quad \tilde{n}_2 + \tilde{n}_M = \tilde{n}_{2,t}. \quad (10)$$

The Bose and Fermi statistics formulas (3) and (4) become

$$\tilde{n}_\alpha = \left[\frac{\tilde{m}_\alpha \tilde{T}}{2\pi} \right]^{3/2} B_{3/2}(-\tilde{\mu}_\alpha/\tilde{T}) + \tilde{n}_\alpha^{(0)} \quad (\text{for boson } A_\alpha), \quad (11)$$

$$\tilde{n}_\alpha = \left[\frac{\tilde{m}_\alpha \tilde{T}}{2\pi} \right]^{3/2} F_{3/2}(-\tilde{\mu}_\alpha/\tilde{T}) \quad (\text{for fermion } A_\alpha). \quad (12)$$

Now the problem of obtaining the atom-molecule equilibrium states is reduced to solving Eqs. (9) and (10) with (11) and (12) for temperature \tilde{T} , molecular binding energy $\Delta\tilde{E}_M$, and mass and total density of A_1 (\tilde{m}_1 , $\tilde{n}_{1,t}$). The scaled atomic masses and the scaled total densities take the values of $0 \leq \tilde{m}_\alpha, \tilde{n}_{\alpha,t} \leq 1$ and satisfy

$$\tilde{m}_1 + \tilde{m}_2 = 1, \quad \tilde{n}_{1,t} + \tilde{n}_{2,t} = 1. \quad (13)$$

These constraints play the role of reducing the number of independent parameters.

III. MOLECULAR FORMATIONS IN NONINTERACTING ATOMIC-GAS MIXTURES

A. Bose-Einstein condensation and Fermi degeneracy

Before presenting the calculational results, we discuss two interesting quantum effects: BEC for bosons and Fermi degeneracy (FD) for fermions.

As discussed in the previous section, the phase transition to the BEC of the boson A_α occurs when $\tilde{\mu}_\alpha = 0$ in (11); the transition temperature T_C is

$$\tilde{T}_C = \frac{2\pi(\tilde{n}_\alpha)^{2/3}}{\tilde{m}_\alpha} [\zeta(3/2)]^{-2/3} \sim 3.313 \frac{(\tilde{n}_\alpha)^{2/3}}{\tilde{m}_\alpha}, \quad (14)$$

where $\zeta(3/2)$ is the Riemann zeta function. The condensed and thermal parts of the number density at $T < T_C$ are given by (11); with scaled quantities, they become

$$\tilde{n}_\alpha^{(th)} = \left(\frac{\tilde{m}_\alpha \tilde{T}}{2\pi} \right)^{3/2} \zeta(3/2), \quad \tilde{n}_\alpha^{(0)} = \left[1 - \left(\frac{\tilde{T}}{\tilde{T}_C} \right)^{3/2} \right] \tilde{n}_\alpha. \quad (15)$$

From these equations, we can find that, if bosons A_α exist in the mixture at $\tilde{T} = 0$ ($\tilde{n}_\alpha \neq 0$), all A_α should condense into the BEC ($\tilde{n}_\alpha^{(0)} = \tilde{n}_\alpha$ at $\tilde{T} = 0$).

Different from bosons, fermions go into the FD state at very low temperatures; especially, at $\tilde{T} = 0$, Eq. (12) becomes

$$\tilde{n}_\alpha = \frac{\sqrt{2}(\tilde{m}_\alpha)^{3/2}}{3\pi^2} (\tilde{\mu}_{F,\alpha})^{3/2}, \quad (16)$$

where $\mu_{F,\alpha} \equiv \tilde{\mu}_\alpha(\tilde{T} = 0)$ is the Fermi energy.

The transition into the FD state is not a phase transition, but a continuous one, so that, different from the BEC \tilde{T}_C in (14), no clear boundaries exist for FD. Instead, as an estimation of the occurrence of FD, we use the temperature at $\tilde{\mu}_{F,\alpha} = 0$:

$$\tilde{T}_{F,\alpha} = \frac{(6\pi^2 \tilde{n}_{F,\alpha})^{2/3}}{2\tilde{m}_{F,\alpha}} \sim 7.569 \frac{(\tilde{n}_\alpha)^{2/3}}{\tilde{m}_\alpha}. \quad (17)$$

Because of the permitted ranges of the scaled densities $0 \leq \tilde{n} \leq 1$, we can find $\tilde{T}_C \sim \tilde{T}_F$ from Eqs. (14) and (17) as a rough estimation; quantum effects begin to appear at the same order of temperature in both noninteracting Bose and Fermi gases.

B. Molecular formations in the BF mixture

Let us consider the BF mixture ($A_1 = B$, $A_2 = F$) with the molecular formation process $B + F \leftrightarrow M = (BF)$. The atom or molecule densities $\tilde{n}_{B,F,M}$ in atom-molecule equilibrium are obtained from the equilibrium condition (9) with Eqs. (10)-(12). Interparticle interaction effects are neglected, which will be discussed in a later section.

To understand the overall structure of the atom-molecule equilibrium, we consider the phase diagram at $T = 0$, which is obtained with analytical calculations as shown in Appendix B. Fig. 1 shows the $T = 0$ phase diagram of the BF mixture with the same atom masses $\tilde{m}_B = \tilde{m}_F = 1/2$ for the molecular binding energy ($\Delta\tilde{E}_M$) and a total density of B ($\tilde{n}_{B,t}$). Because of the constraints (13), $\Delta\tilde{E}_M$ and $\tilde{n}_{B,t}$ are unique parameters to determine the equilibrium state. The bracketed letters in the regions or lines in Fig. 1 represent the species which exist in equilibrium at $T = 0$; for example, (B, F, M) in the central region means that atoms B and F and molecule M coexist there, etc.

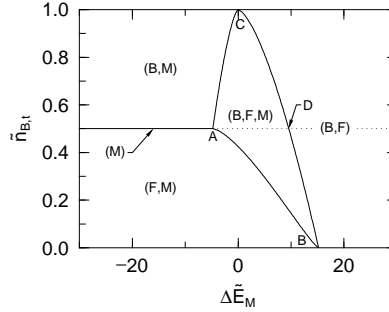


FIG. 1: The $T = 0$ phase diagram of BF mixtures with the same atom masses in the $\Delta\tilde{E}_M$ - $\tilde{n}_{B,t}$ plane. The bracketed letters show what kinds of particles exist in equilibrium at $T = 0$.

From Fig. 1, we find that the BF mixture at $T = 0$ shows the structure that, in the area left of the border BAC ($\Delta\tilde{E}_M \lesssim 0$), the states with molecules as many as possible become stable (molecular states) and, in the area right of the boundary BC , all molecules dissociate into atoms B and F (dissociated states). Between these two areas, mixed states of atoms and molecules become stable in the sense of equilibrium.

In Fig. 1, we can read off the existence condition of the BEC of atom B ; it is in the regions with the bracketed B because the bosons always condense into a BEC at $T = 0$.

We now turn to the atom-molecule equilibrium of the BF mixture at finite temperatures, which are obtained in numerical calculations using (4) and (9). Fig. 2 shows the temperature

dependences of the scaled densities \tilde{n}_B and \tilde{n}_M in the BF mixture with masses $\tilde{m}_B = \tilde{m}_F = 1/2$ and the same total atomic-number densities $\tilde{n}_{B,t} = \tilde{n}_{F,t} = 1/2$. The lines d , e , and f in Fig. 2 are for several values of the molecular binding energies: $\Delta\tilde{E}_M = 0$, -4.78 , and 9.57 , respectively. The BEC line (14) and the $\tilde{\mu}_F = 0$ line, Eq. (17), are also drawn in Fig. 2 as lines a and b , respectively; they show the boundaries where quantum-statistical effects begin to occur.

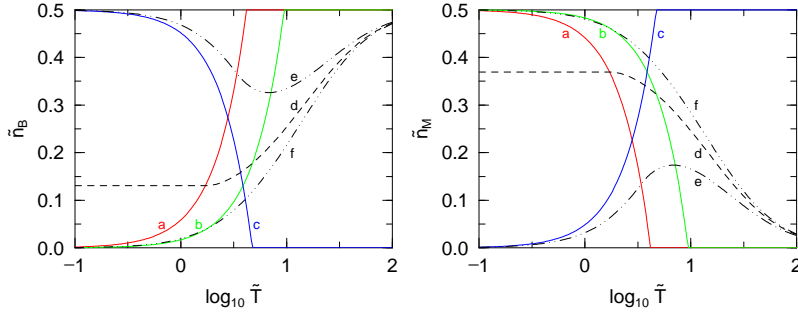


FIG. 2: (Color online) Temperature dependences of the number densities \tilde{n}_B of the bosonic atom B [(a), left] and \tilde{n}_M of the molecule M [(b), right] in the BF mixture with the same atomic masses and the same total atomic densities. The lines d (dashed line), e (double-dot-dashed line) and f (triple-dot-dashed line) are for mixtures with $\Delta\tilde{E}_M = 0$, 9.57 (resonance state), and -4.78 (bound state), respectively. The BEC T_C line of B (line a) and the $\tilde{\mu}_F = 0$ lines for F (line b) and M (line c) are also drawn.

Fig. 2 shows that, at the high-temperature limit, \tilde{n}_M converge to 0 (complete dissociation of molecules into atoms). It can be explained by the energy-entropy balance in the free energy. The atom-molecule mixed states have a reduction in the energy part of the free energy; in contrast, the dissociated states have a reduction of the entropy part because the state density of $B + F$ is larger than that of molecules. With increasing temperature, the entropy contribution becomes large and the reaction process swings to the dissociation of molecules. This mechanism can also be applied to BB or FF mixtures because the binding energy and quantum-statistical properties are less effective at high temperature.

The equilibrium states have a large dependence on the binding energy $\Delta\tilde{E}_M$ around and below the BEC T_C and $\tilde{\mu}_F = 0$ lines. At $T = 0$, they converge to states belonging to the phases on the horizontal $\tilde{n}_{F,t} = 1/2$ line in Fig. 1: the molecular, mixed and dissociated phases divided by the points, $\Delta\tilde{E}_M = \Delta_1 \equiv -(3\pi^2)^{2/3}/2 \approx -4.78$ (point A) and $\Delta_2 \equiv$

$(3\pi^2)^{2/3} \approx 9.57$ (point D). The temperature dependence in Fig. 2 is also classified with the values of $\Delta\tilde{E}_M$: (i) $\Delta\tilde{E}_M \leq \Delta_1$ (lines f). With decreasing T , the \tilde{n}_B becomes small and goes below the BEC T_C line (no BEC of atom B for all temperatures). (ii) $\Delta_1 < \Delta\tilde{E}_M < \Delta_2$ (line d). With decreasing T , \tilde{n}_B (and also \tilde{n}_F) and \tilde{n}_M run into the BEC and $\tilde{\mu} \geq 0$ regions, and converge into finite values. (iii) $\Delta_2 \leq \Delta\tilde{E}_M$ (line e). With decreasing T , \tilde{n}_M takes the maximum value on the right of the $\tilde{\mu} = 0$ line (line c) and decreases to $\tilde{n}_M = 0$ along the line from below.

The atom-molecule equilibrium in the BF mixtures can be explained by competition between the quantum-statistical effects and the binding energy of M ; the molecule states give a free-energy reduction because of $\Delta\tilde{E}_M < 0$, but at low T , the molecules constitute the FD states, which have large kinetic energies coming from the occupied high-energy one-particle states. In contrast, in dissociated states, in spite of the kinetic-energy contribution from the FD states of the fermions F , the bosons B can reduce the kinetic energy largely as they condense into the BEC at low- T . Thus, depending on the positive or negative value of $\Delta\tilde{E}_M$, the dissociated or molecular state becomes stable, and a mixed phase appears between them.

C. Molecular formations in the FF mixture

In the FF mixture ($A_1 = F1$, $A_2 = F2$), we consider atom-molecule equilibrium through the process $F1 + F2 \leftrightarrow M = (F1F2)$ in the same way as in the BF mixture. In this section, we take the FF mixture with the same atomic masses $\tilde{m}_{F1} = \tilde{m}_{F2} = 1/2$.

Fig. 3 shows the $T = 0$ phase diagram of the FF mixture. The notation for each phase is the same as that of the BF mixture (see Fig. 1). Analytical expressions of the phase-boundary lines and points in Fig. 3 are given in Appendix B.

The topological structure of the equilibrium phases in Fig. 3 is the same as that in the BF mixture (Fig. 1); it consists of a “molecular phase” to the left of the border BAC , a “dissociated phase” to the right of the boundary BC , and a “mixed phase” between them.

The existence condition of BEC of the bosonic molecules M is also read off in Fig. 3 as the regions with the symbol M in brackets.

The equilibrium states at $T \neq 0$ can be expressed in the same way as in the BF mixture. In Fig. 4, we show the temperature dependences of \tilde{n}_{F1} and \tilde{n}_M in the FF mixture with

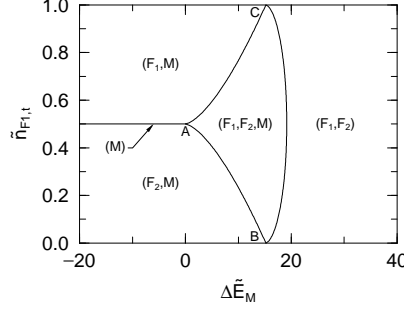


FIG. 3: The $T = 0$ phase diagram of the FF mixture with the same atom masses in the $\Delta\tilde{E}_M - \tilde{n}_{F1,t}$ plane. The bracketed letters show what kinds of particles exist in equilibrium at $T = 0$.

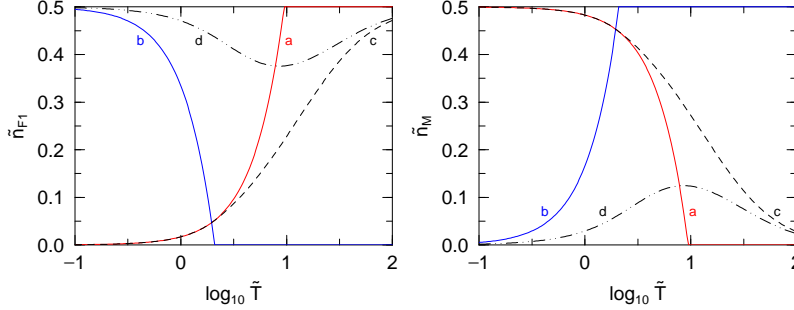


FIG. 4: (Color online) Temperature dependences of the number densities \tilde{n}_{F1} of the atom $F1$ [(a), left] and \tilde{n}_M of the molecule M [(b), right] in the FF mixture with the same atomic masses and the same total atomic densities. The lines c (dashed line) and d (double-dot-dashed line) are for mixtures with $\Delta\tilde{E}_M = 0$ and 19.1 (resonance state), respectively. The $\tilde{\mu}_F = 0$ lines and the BEC T_C lines are drawn for $F1$ and $F2$ (line a) and M (line b).

$\tilde{n}_{F1,t} = \tilde{n}_{F2,t} = 1/2$ (the states on the line $\tilde{n}_{F1,t} = 1/2$ in Fig. 3) and $\Delta\tilde{E}_M = 0$ and 19.1. In the FF mixture, the $T = 0$ phases are classified with the value of $\Delta\tilde{E}_M$: (i) $\Delta\tilde{E}_M < 0$ (molecule phase), (ii) $0 < \Delta\tilde{E}_M < \Delta_3$ (mixed phase), and (iii) $\Delta_3 < \Delta\tilde{E}_M$ (dissociated phase), where the border points with $\Delta\tilde{E}_M = 0$ and $\Delta_3 \equiv 2(3\pi^2)^{2/3} \approx 19.1$ correspond to point A and the crossing point between line BC and $\tilde{n}_{F1,t} = 1/2$ in Fig. 3. The two lines c and d in Fig. 4 are for the border between two phases.

We should comment on the relation of the present approach to the FF mixture with the BEC-BCS crossover theory[21, 22, 23]. In the crossover theory, two kinds of bare fermions become dressed quasifermions, and quasimolecule states (or Cooper-pair states) appear as physical degrees of freedoms. The strength change of the attraction between bare

fermions gives the crossover between the BCS states (weak interaction) and the molecular BEC states (strong interaction). In the present quasiequilibrium approach, the fermions and the molecule should be considered as quasi-particles; the effects of bare-particle interactions are included as the existence of the molecule and its binding energy $\Delta\tilde{E}_M$. Really, the present approach is proved to give an approximated result on the strong interaction (BEC) side ($\Delta\tilde{E}_M \lesssim 0$) [21]. In the weak interaction (BCS) side, the BEC \tilde{T}_C in the present approach vanishes at $\Delta\tilde{E}_M = \Delta_3$ as shown in Fig. 3 and disagrees with the BCS T_C . This is because the molecule states are treated as structureless bosons and no statistical correlations are introduced. It can be said that the present approach should give a good approximation in the strong interaction side and in the high- T region.

D. Molecular formations in the BB mixture

Before discussing the results, we should give some explanations of the singular property of the boson chemical potential at the double limit of $n_B = 0$ and $T = 0$ in the no BEC region.

Around the point of $(n_B, T) \sim (0, 0)$, $\nu = -\mu_B/k_B T$ becomes large, so that the Bose function $B_{3/2}$ in the density formula (6) can be approximated by an asymptotic formula [Eq. (A9) in Appendix A]: then the chemical potential becomes

$$\mu_B = k_B T \ln(\lambda_T^3 n_B) \quad (18)$$

with $\lambda_T \propto T^{-1/2}$ defined in (5). Eq. (18) shows that μ_B is singular at $(n_B, T) \sim (0, 0)$ and can take any negative value μ_0 if we take the limit through the pass $n_B \sim (\lambda_{T,B})^{-3} e^{\mu_0/k_B T}$.

Now let us go ahead to the atom-molecule equilibrium in the BB mixture through the process $B1 + B2 \leftrightarrow M = (B1B2)$; then, the equilibrium condition (9) becomes

$$\tilde{\mu}_{B1} + \tilde{\mu}_{B2} - \tilde{\mu}_M = \Delta\tilde{E}_M. \quad (19)$$

If all bosons condense into the BEC, the chemical potentials vanish, $\mu_{B1,B2,M} = 0$, at $T = 0$; it gives a contradiction in (19) except for the case of $\Delta\tilde{E}_M = 0$ (no triple BEC theorem)[48]. The negativeness of the chemical potentials determines the solutions of (19) at $T = 0$: (i) $\Delta\tilde{E}_M < 0$ (molecular phase): $\tilde{\mu}_M = 0$ (the BEC of M) and $\tilde{\mu}_\alpha = \Delta\tilde{E}_M$ with $\tilde{n}_\alpha = 0$ ($\alpha = B1$ or $B2$). (ii) $\Delta\tilde{E}_M > 0$ (dissociated phase): $\tilde{\mu}_{B1} = \tilde{\mu}_{B2} = 0$ (the BECs of $B1$ and $B2$) and

$\tilde{\mu}_M = -\Delta\tilde{E}_M$ with $\tilde{n}_M = 0$. The results are summarized in the $T = 0$ phase diagram in Fig. 5. We should find that no triple BEC states exist except for the states on the boundary line of $\Delta\tilde{E}_M = 0$. Accordingly no mixed phase exists in the BB mixture.

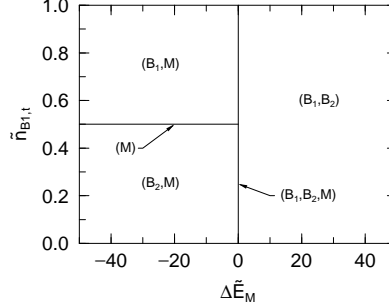


FIG. 5: The $T = 0$ phase diagram of BB mixtures in the $\Delta\tilde{E}_M$ - $\tilde{n}_{B1,t}$ plane. The bracketed letters show what kinds of particles exist in equilibrium at $T = 0$.

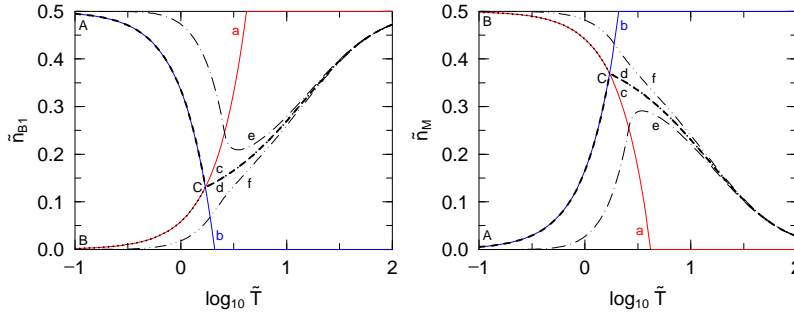


FIG. 6: (Color online) Temperature dependences of the number densities \tilde{n}_{B1} of the atom $B1$ [(a), left] and \tilde{n}_M of the molecule M [(b), right] in the BB mixture with the same atomic masses and the same total atomic densities. The lines c (short-dashed line), d (dotted line), e (dot-dashed line) and f (double-dot-dashed line) are for mixtures with $\Delta\tilde{E}_M = +0, -0, +1$, and -1 , respectively, where $\Delta\tilde{E}_M = \pm 0 \equiv \lim_{\epsilon \rightarrow +0} \pm \epsilon$. The BEC T_C lines of $B1$ and $B2$ (line a) and M (line b) are also drawn.

Fig. 6 shows the temperature dependences of \tilde{n}_{B1} and \tilde{n}_M in the BB mixture with $\tilde{m}_{B1} = \tilde{m}_{B2} = 1/2$ and $\tilde{n}_{B1,t} = \tilde{n}_{B2,t} = 1/2$ (the states on the line $\tilde{n}_{B1,t} = 1/2$ in Fig. 5) for $\Delta\tilde{E}_M = \pm 0, \pm 1$. The above-mentioned exclusive behaviors at $T = 0$ for BEC have influences also at $T \neq 0$ as shown in Fig. 6: in $\Delta\tilde{E}_M < 0$, only the molecules become the BEC (lines e); otherwise, only atomic BECs can occur (lines f). The mixture with $\Delta\tilde{E}_M = 0$ has a

singularity at point C ; if we take the different kinds of limit $\Delta\tilde{E}_M = \pm 0$, BEC of atoms or molecules occurs, respectively.

The exclusiveness between atom and molecule BECs in BB mixtures has been observed in a Cs experiment by the Innsbruck group[9]; a sudden interchange occurs between the atom and molecule BECs when the resonance becomes the bound molecule using the Feshbach resonance method. This observation shows that the exclusiveness is incomplete and some mixture of atom and molecule BECs exists on the bound molecule side; it might be explained by an interparticle interaction effect (see Sec. V) or nonequilibrium effect.

IV. LAW OF QUANTUM MASS ACTION

In mixtures of classical Maxwell-Boltzmann gases, the molecular formation or dissociation processes through (1) satisfy the “law of mass action”:

$$\frac{n_1 n_2}{n_M} = K(T), \quad (20)$$

where $n_{1,2,M}$ are the number densities of the particle $A_{1,2,M}$ and $K(T)$ is an equilibrium constant, which depends on T , but not on $n_{1,t}$ and $n_{2,t}$.

In the present calculations of ultracold molecular formation or dissociation processes, quantum-statistical effects play an important role, so that they give the density dependence of $K(T)$ in (20); we call it the “law of quantum mass action”.

In order to make a comparison with the quantum cases, we derive an exact form of (20) in the case of ideal Maxwell-Boltzmann gases, where the density of the particle A_α is given by

$$n_\alpha^{(MB)} = \lambda_{T,\alpha}^{-3} e^{\mu_\alpha/k_B T}, \quad (21)$$

with the thermal de Broglie wave length defined in (5). Substituting Eq. (21) into the equilibrium condition (2), we obtain the classical law of mass action [43, 49]:

$$\frac{n_1^{(MB)} n_2^{(MB)}}{n_M^{(MB)}} = \left(\frac{\lambda_{T,M}}{\lambda_{T,1} \lambda_{T,2}} \right)^3 e^{\Delta G/k_B T} \equiv K(T), \quad (22)$$

where ΔG is called the standard chemical affinity, and it becomes $\Delta G = \Delta E_M$ (the binding energy of the molecule A_M).

To show the deviations from the law of quantum action by quantum effects, we evaluate the ratio of $n_1 n_2 / n_M$ calculated in the previous section (including the quantum effects) to

$n_1^{MB} n_2^{MB} / n_M^{MB} = K(T)$ given by (22):

$$R \equiv \frac{n_1 n_2}{n_M} \frac{n_M^{(MB)}}{n_1^{(MB)} n_2^{(MB)}} = \frac{n_1 n_2}{n_M} \frac{1}{K(T)}. \quad (23)$$

The ratio R generally depends on \tilde{T} and $\tilde{n}_{1,t}$ because of the constraint (13).

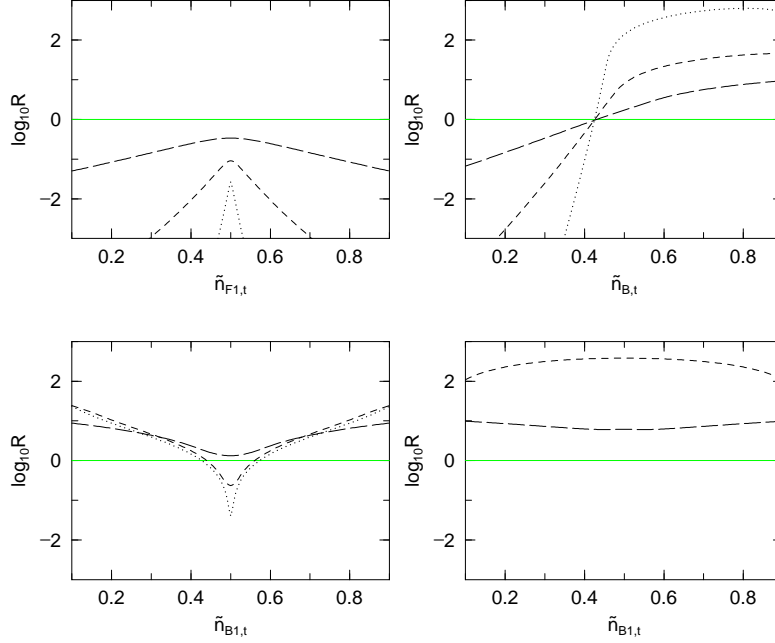


FIG. 7: (Color online) The ratio R defined by (23) for the FF [(a), top left], BF [(b), top right], and BB [(c) and (d), bottom left and right] mixtures with the same atom masses. The mass defects are $\Delta\tilde{m}_M = -1$ for the FF and BF mixtures and $\Delta\tilde{m}_M = -1$ (c), $+1$ (d) for the BB mixtures. The lines are for temperatures: $\log_{10} \tilde{T} = \infty$ (Maxwell-Boltzmann limit, solid line), 0.4 (long-dashed line), 0 (short-dashed line), and -0.4 (dotted line), respectively.

In Fig. 7, we show the $\tilde{n}_{1,t}$ dependences of $\log R$ for several temperatures ($\log \tilde{T} = -0.4, 0, 0.4, \infty$) in the case of FF, BF, and BB mixtures with $\tilde{m}_1 = \tilde{m}_2 = 1/2$. The mass defects are $\Delta\tilde{m}_M = -1$ for the FF and BF mixtures and $\Delta\tilde{m}_M = +1$ [Fig. 7(c)] and -1 [Fig. 7(d)] for the BB mixtures. In the BB mixture, the behaviors of R are found to be very different for molecules and resonances.

To understand the deviations from the law of mass action, we expand the ratio R in the high- T region analytically:

$$R_{BB} \sim 1 + \frac{1}{2^{3/2}} \left(-\lambda_{T,1}^3 n_1 - \lambda_{T,2}^3 n_2 + \lambda_{T,M}^3 n_M \right), \quad (24)$$

$$R_{FF} \sim 1 + \frac{1}{2^{3/2}} \left(+\lambda_{T,1}^3 n_1 + \lambda_{T,2}^3 n_2 + \lambda_{T,M}^3 n_M \right), \quad (25)$$

$$R_{BF} \sim 1 + \frac{1}{2^{3/2}} \left(-\lambda_{T,1}^3 n_1 + \lambda_{T,2}^3 n_2 - \lambda_{T,M}^3 n_M \right), \quad (26)$$

where $R_{BB,FF,BF}$ are for the BB,FF,BF mixtures. The leading-order terms $R \sim 1$ in Eqs. (24)-(26) correspond to the Maxwell-Boltzmann limit (law of mass action). Completely different contributions are found in the next-order terms ($\propto T^{-3/2}$) for R_{BB} and R_{FF} in BB and FF mixtures, which are consistent with the results in Fig. 7(a) and Figs. 7(c) and 7(d) at high T . The relatively small T dependence of the ratio R_{BF} for the BF mixture [Fig. 7(b)] at high T can be explained quantitatively from the cancellation of the boson and fermion contributions in the $T^{3/2}$ term in (26).

V. EFFECTS OF INTERPARTICLE INTERACTIONS ON EQUILIBRIUM

A. Interaction effects in the mean-field approximation

In the previous sections, we discussed atom-molecule equilibrium in noninteracting atom-gas mixtures. If interactions exist between atom-atom, atom-molecule, and molecule-molecule (interacting) mixtures, they should modify the equilibration and sufficiently strong interactions could change the phase structures of the mixtures.

Theoretically, the effects of the interactions for the free energy can be divided into two kinds: mean-field and correlation ones. The mean-field effect can be evaluated, for example, using the Hartree-Fock approximation, and it can be represented as interaction terms (background energy) in the one-particle energies of atoms or molecules in the mixtures. The correlation effects are defined as the contributions that cannot be introduced in the mean-field approximation. It should be noted that this division of interaction effects is a theoretical one and sometimes ambiguous. For example, in the BCS theory of superconductors, if we take the normal quasielectron theory of a normal Fermi-degenerate vacuum in the Hartree-Fock sense, then Cooper pairs and their condensations are created by correlation effects; however, if we take the Bogoliubov quasi-particles as dynamical degrees of freedom, the BCS states can be understood as a kind of mean-field theory. In this paper, we discuss interaction effects for atom-molecule equilibrium in the Hartree-Fock-like mean-field approximation.

For interparticle interactions, we take the ones coming through the two-body s -wave scattering processes, which give dominant contributions in ultracold atomic gases except the strongly interacting or spin-degenerate ones. They can be introduced through effective interactions, for which we use the pseudopotentials[50]

$$V_{i,j} = g_{i,j} \sum_{\alpha,\beta} \delta^3(\mathbf{r}_\alpha - \mathbf{r}'_\beta), \quad (i, j = A1, A2, M) \quad (27)$$

between the α th and β th particles of the i and j species, respectively. The coupling constants $g_{i,j}$ are determined from the s -wave scattering lengths $a_{i,j}$ between i and j species:

$$g_{i,j} = \frac{2\pi\hbar^2}{\mu_{i,j}} a_{i,j}, \quad (28)$$

where $\mu_{i,j} \equiv m_i m_j / (m_i + m_j)$ is the reduced mass.

Let us consider the contributions of the interactions in mixtures with equilibrium $A1 + A2 \leftrightarrow M$ in the mean-field approximation.

The interaction effects are introduced into the free energy as the background energy:

$$F = E_0 + E^{int} - \sum_{i=A1,A2,M} \mu_i n_i, \quad (29)$$

where the E_0 is the kinetic energy, which exists also in noninteracting cases.

The contribution of the potential $V_{i,j}$ in (27) to the background energy E^{int} is evaluated by $E_{i,j}^{int} = \langle V_{i,j} \rangle$. In the mean-field approximation, it is expressed by the number densities n_i and n_j . In the interaction between the same kinds of particles, it becomes

$$E_{BB} = \frac{g_{BB}}{2} \{2n_B^2 - (n_B^{(0)})^2\}, \quad E_{FF} = 0, \quad (30)$$

for the boson B and the fermion F . The $n_B^{(0)}$ is the condensed density of B ; when $T \sim 0$, we can use the approximation that $n_B^{(0)} \sim n_B$. The vanishing background energy for the fermion F originates in forbidden s -wave scatterings by Pauli blocking effects at $T \sim 0$. To avoid unnecessary complexity in the formulation, we redefine $g_{FF} = 0$ for the fermions. The background energies coming from the interactions between different kinds of particles become

$$E_{i,j} = g_{i,j} n_i n_j \quad (i \neq j). \quad (31)$$

From the above considerations, the total background energy in the equilibrium through $A1 + A2 \leftrightarrow M$ can be approximated by

$$E^{int} = \sum_{i=A1,A2,M} \frac{g_{i,i}}{2} (n_i)^2 + g_{A1,A2} n_{A1} n_{A2} + g_{A1,M} n_{A1} n_M + g_{A2,M} n_{A2} n_M. \quad (32)$$

Differentiating the free energy F in (29) with respect to the density n_i , we obtain the single-particle energy

$$\epsilon_i = \epsilon_i^{(0)} + \sum_{j=A1,A2,M} g_{i,j} n_j - \mu_i, \quad (33)$$

where $\epsilon_i^{(0)}$ is the kinetic energy of particle i :

$$\epsilon_i^{(0)} = \frac{\partial E_0}{\partial n_i} = \frac{(\mathbf{p}_i)^2}{2m_i}. \quad (34)$$

With the effective chemical potential defined by

$$\mu'_i = \mu_i - \sum_{j=A1,A2,M} g_{i,j} n_j, \quad (35)$$

Eq. (33) becomes

$$\epsilon_i = \epsilon_i^{(0)} - \mu'_i. \quad (36)$$

It should be noticed that the ϵ_i in (36) has the same form as that in the noninteracting case, so that the same Bose and Fermi statistic formulas (11) and (12) can be applied also in the interacting case using the effective chemical potential μ'_i instead of μ_i :

$$\tilde{n}_\alpha = \left[\frac{\tilde{m}_\alpha \tilde{T}}{2\pi} \right]^{3/2} B_{3/2}(-\tilde{\mu}'_\alpha / \tilde{T}) \quad (\text{for boson } A_\alpha), \quad (37)$$

$$\tilde{n}_\alpha = \left[\frac{\tilde{m}_\alpha \tilde{T}}{2\pi} \right]^{3/2} F_{3/2}(-\tilde{\mu}'_\alpha / \tilde{T}) \quad (\text{for fermion } A_\alpha). \quad (38)$$

Using eq. (35), the equilibrium condition (9) for the interacting mixture becomes

$$\mu'_{A1} + \mu'_{A2} - \mu'_M = \Delta E'_M, \quad (39)$$

where the effective binding energy $\Delta E'_M$ is given by the density of the M molecule

$$\Delta E'_M = \alpha n_M + \gamma, \quad (40)$$

where interaction effects are included in the two parameters α and γ :

$$\alpha = \sum_{i=A1,A2,M} g_{i,i} + 2(g_{A1,A2} - g_{A1,M} - g_{A2,M}), \quad (41)$$

$$\gamma = \Delta E + (g_{A1,M} - g_{A1,A1} - g_{A1,A2})n_{A1,t} + (g_{A2,M} - g_{A2,A2} - g_{A1,A2})n_{A2,t}. \quad (42)$$

In the derivation of eqs. (40)-(42), we have used the constraints (13).

As has been done in the case of noninteracting mixtures in Sec. IIB, we introduce scaled variables for the coupling constants and the effective binding energies:

$$\tilde{g}_{i,j} = \frac{g_{i,j}n_t}{E_s}, \quad (43)$$

$$\Delta\tilde{E}'_M = \frac{\Delta\tilde{E}'_M}{E_s}, \quad (44)$$

where $n_t = n_{1,t} + n_{2,t}$ and $E_s = \hbar^2(n_t)^{2/3}/m_M$. For the effective binding energy $\Delta\tilde{E}'_M$, Eq. (40) becomes

$$\Delta\tilde{E}'_M = \tilde{\alpha}\tilde{n}_M + \tilde{\gamma}, \quad (45)$$

where the scaled parameters $\tilde{\alpha}$ and $\tilde{\gamma}$ are defined by

$$\tilde{\alpha} = \sum_{i=A1,A2,M} \tilde{g}_{i,i} + 2(\tilde{g}_{A1,A2} - \tilde{g}_{A1,M} - \tilde{g}_{A2,M}), \quad (46)$$

$$\tilde{\gamma} = \Delta\tilde{E} + (\tilde{g}_{A1,M} - \tilde{g}_{A1,A1} - \tilde{g}_{A1,A2})\tilde{n}_{A1,t} + (\tilde{g}_{A2,M} - \tilde{g}_{A2,A2} - \tilde{g}_{A1,A2})\tilde{n}_{A2,t}. \quad (47)$$

Using the scaled variables, the atom-molecule equilibrium condition (39) becomes

$$\tilde{\mu}_1 + \tilde{\mu}_2 - \tilde{\mu}_M = \Delta\tilde{E}'_M \equiv \tilde{\alpha}\tilde{n}_M + \tilde{\gamma}, \quad (48)$$

where Eq. (45) has been used.

The atom-molecule equilibrium states of the interacting mixtures can be obtained from eqs. (37)-(39) with the constraints (13). The interaction effects are included in the effective binding energy $\Delta E'_M$ in (40) through the two parameters α and γ , which are determined from the coupling constants $g_{i,j}$. Thus, we find that, in the mean-field approximation, one extra parameter is necessary in the equilibrium theory of interacting mixtures in comparison with that of noninteracting ones.

B. Phase structure changes by interaction effects

Before we give the numerical results for the atom-molecule equilibrium states of the interacting mixtures, we discuss qualitatively how the interactions shift and change the phase structures (PSs). We assume that all coupling constants are positive $g_{i,j} > 0$ to avoid possible instabilities from the spatial fluctuations of densities[38].

Different from noninteracting cases where the equilibrium condition (9) has a unique solution, the existence of the density-dependent term $\tilde{\alpha}\tilde{n}_M$ in (48) results in two or more

different solutions of (48), which correspond to the different equilibrium states (coexisting phases). These solutions include locally stable and unstable states, so that we have to examine the behavior of Eq. (48) and take out solutions corresponding to stable states.

Close examination shows that two critical points $0 > \tilde{\alpha}_{c1} > \tilde{\alpha}_{c2}$ exist in the parameter $\tilde{\alpha}$ for the BF, FF, and BB mixtures, and the $T = 0$ equilibrium structures can be classified into three regions with them as folloes,

PS1 ($\tilde{\alpha}_{c1} < \tilde{\alpha}$), Eq. (48), has unique solutions for each value of the parameters $\tilde{\alpha}$, $\tilde{\gamma}$, and $\tilde{n}_{1,2,t}$, and the $T = 0$ phase diagrams become similar in structure with those for the noninteracting mixtures, including the dissociate, mixed, and molecule phases. (As shown later, the BB mixture is somewhat exceptional.)

PS2 ($\tilde{\alpha}_{c2} < \tilde{\alpha} < \tilde{\alpha}_{c1}$), Eq. (48), has two stable (one unstable) solutions in the mixed phase.

PS3 ($\tilde{\alpha} < \tilde{\alpha}_{c2}$) has new coexisting phases appearing where both the mixed and molecular states become locally stable.

Thus, interaction effects generally give complex phase structures in atom-molecule equilibrium with the phases with two locally stable states. The occurrence of these phases depends on the parameters $\tilde{\alpha}$, $\tilde{\gamma}$, and $\tilde{n}_{1,2,t}$, and the transitions of the states caused by the change of these parameters might be first order. In the phases with two locally stable states, the absolutely stable equilibrium state should be determined from a free-energy comparison of these states. However, the difference of the free energies of these states is generally small, so that effects that are not included in the present mean-field calculations (the correlation effect) may give comparative contributions, and, also, in real experiments, states which are not absolutely stable can occur through nonequilibrium and history effects. For these reasons, we should say that the stability of these phases is very subtle, and a study of the more detailed structures of these phases will not be done in this paper.

From Eq. (46), the negative contributions to $\tilde{\alpha}$ can be given by large values of $\tilde{g}_{A1,M}$ and $\tilde{g}_{A2,M}$; thus, atom-molecule interactions are found to be interesting and important in transitions to unstable phases.

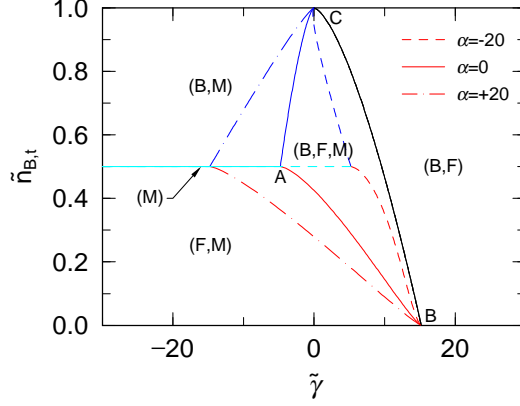


FIG. 8: (Color online) The $T = 0$ phase diagram of interacting BF mixtures with the same atom masses in the $\tilde{\gamma}$ - $\tilde{n}_{B,t}$ plane for $\tilde{\alpha} = -20, 0, 20$. The bracketed letters in the regions or lines show what kinds of particles exist in equilibrium at $T = 0$.

C. Phase structures of the interacting BF mixture

The critical values $\tilde{\alpha}_{c1}^{(BF)}$ and $\tilde{\alpha}_{c2}^{(BF)}$ for the BF mixture are given by

$$\tilde{\alpha}_{c1}^{(BF)} = -\frac{2^{4/3}}{3} \left(\frac{3\pi^2}{\sqrt{2}} \right)^{2/3} \left[1 + \frac{1}{2^{1/4} \tilde{m}_F^{3/4}} \right], \quad (49)$$

$$\tilde{\alpha}_{c2}^{(BF)} = -2^{1/3} \left(\frac{3\pi^2}{\sqrt{2}} \right)^{2/3} \left[1 + \frac{1}{\tilde{m}_F} \right]. \quad (50)$$

Fig. 8 shows the $T = 0$ phase diagram for interacting BF mixtures with $\tilde{m}_B = \tilde{m}_F = 1/2$

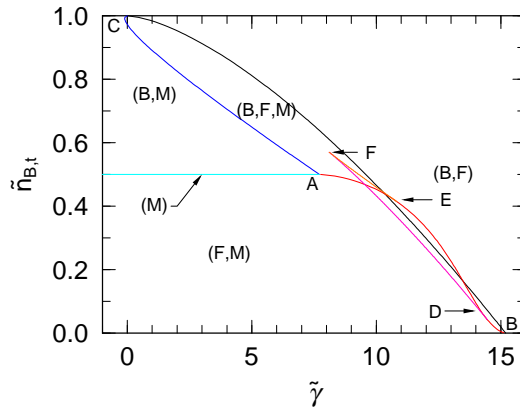


FIG. 9: (Color online) The $T = 0$ phase diagram of interacting BF mixtures with the same atom masses in the $\tilde{\gamma}$ - $\tilde{n}_{B,t}$ plane for $\tilde{\alpha} = -25$. The bracketed letters in the regions or lines show what kinds of particles exist in equilibrium at $T = 0$.

for $\tilde{\alpha} = -20, 0, 20$. Eqs. (49) and (50) give $\tilde{\alpha}_{c1}^{(BF)} \sim -20.7$ and $\tilde{\alpha}_{c2}^{(BF)} \sim -28.7$ when $\tilde{m}_B = \tilde{m}_F = 1/2$, so that the phase diagrams in Fig. 8 are found to show the phase structure PS1; they have qualitatively similar structures as the diagram for the noninteracting mixture (Fig. 1). Especially, the phase diagram for $\tilde{\alpha} = 0$ (solid line in Fig. 8) is completely the same as that in Fig. 1 because of the vanishing density-dependent term $\tilde{\alpha}\tilde{n}_M$ in (48). We also find that the boundary between the dissociate and mixed phases, CB , in Fig. 8, which is given by (B17) in Appendix B, is independent of the values of $\tilde{\alpha}$; this is because the $n_M = 0$ condition on this boundary eliminates the $\tilde{\alpha}$ dependence in (48). The boundaries between the mixed and molecular phases depend on $\tilde{\alpha}$ as shown in (B15) and (B18) in Appendix B. The $\tilde{\alpha}$ -dependence of the mixed phase can be understood from the position of the end point A in Fig. 8:

$$\tilde{\gamma} = -\left(\frac{3\pi^2}{2\sqrt{2}}\right)^{2/3} - \frac{\tilde{\alpha}}{2} \sim -4.78 - \frac{\tilde{\alpha}}{2}, \quad (51)$$

which is given by (B20) in Appendix B. Eq. (51) shows that the area of the mixed phase increases when $\tilde{\alpha} > 0$ and decreases in the case of $\tilde{\alpha} < 0$. This behavior can be explained from (48); in the case of $\tilde{\alpha} > 0$, the molecule density \tilde{n}_M has the effect of increasing $\Delta\tilde{E}'_M$, which makes molecular formation difficult, and the area of the mixed phase becomes large (the $\tilde{\alpha} < 0$ case has the contrary effect).

The phase diagrams with the phase structures PS2 and PS3 are given in Fig. 9 ($\tilde{\alpha} = -25$) and Fig. 10 ($\tilde{\alpha} = -30$). In Fig. 9, the occurrence of two locally stable states gives the additional two phases with the boundaries $(AB + DF)$ and $(DF + AB + EF)$. The areas of these new phases in the PS2 structure are small; they are nothing more than substructures in the mixed phase. In the PS3 structure (Fig. 10), the left-shifted phase boundary AB crosses the boundary BC , and new kinds of phase can be produced between AB and BC : region (b) in Fig. 10, for example, where dissociated and mixed states coexist. Fig. 10 also has a very complex substructure around the boundary BC . For extremely large values of $\tilde{\alpha}$ (Fig. 11, $\tilde{\alpha} = -70$), the regions with substructures shrink to the small areas around the vertexes B and C in Fig. 11, and the whole phase structure becomes simple again; the phases where the dissociated and molecular states coexist appear in the central region, where the dissociated states include no molecule and the molecular states have as many molecules as possible.

D. Phase structures of interacting BB and FF mixtures

In this subsection, we briefly sketch the structures of the $T = 0$ phase diagrams of interacting BB and FF mixtures.

The $T = 0$ phase diagrams of interacting BB mixtures with $\tilde{m}_{B1} = \tilde{m}_{B2} = 1/2$ are shown in Fig. 12(a) ($\tilde{\alpha} = 20$) and Fig. 12(b) ($\tilde{\alpha} = -20$). In the case of $\tilde{\alpha} > 0$, the phase diagrams have the mixed phases [the region ABC in Fig. 12(a)], which do not exist in the noninteracting cases. The position of the end point A is given by (B25) in Appendix B:

$$\tilde{\gamma} = -\frac{\tilde{\alpha}}{2}, \quad (52)$$

which locates on the left side of the boundary BC in Fig. 12(a). We can understand that

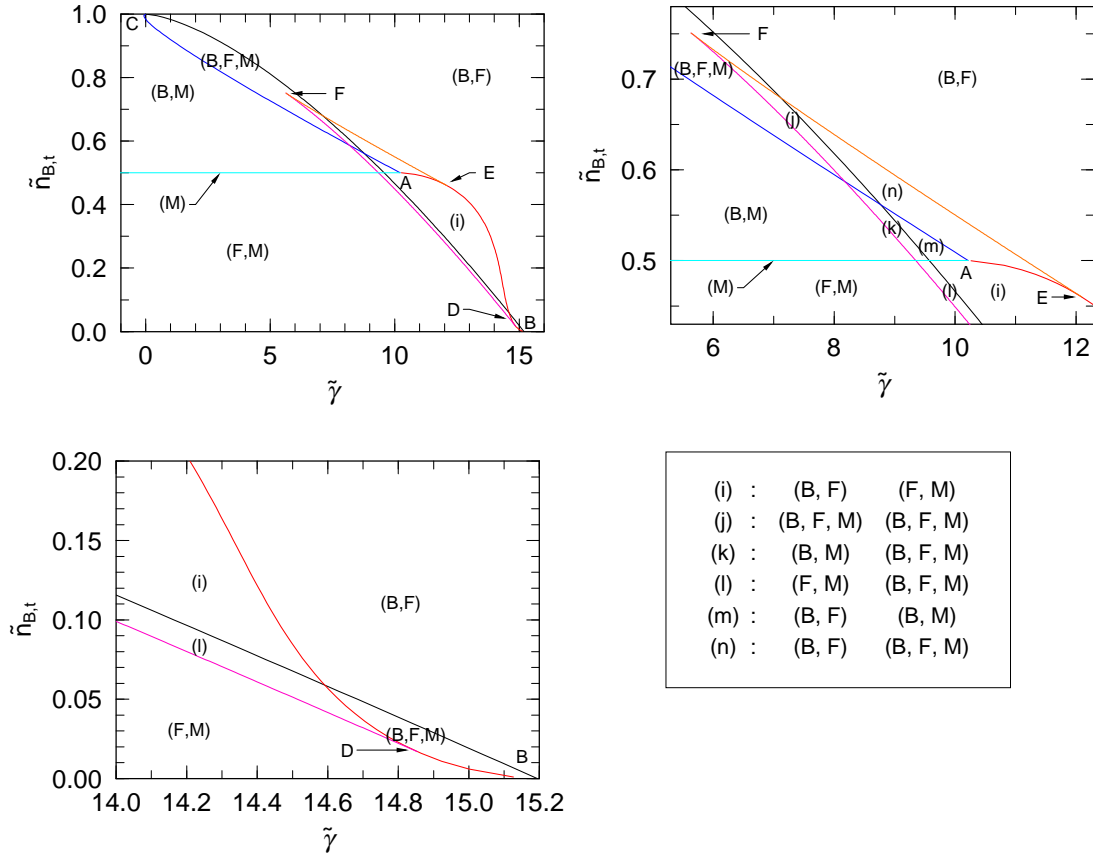


FIG. 10: (Color online) The $T = 0$ phase diagram of interacting BF mixtures with the same atom masses in the $\tilde{\gamma}$ - $\tilde{n}_{B,t}$ plane for $\tilde{\alpha} = -30$ [(a), top left]. (b) and (c) (top right and bottom left) show the detailed structures of (a). (d) (bottom left) is the legend that explains the phases (i)-(n) in (a)-(c).

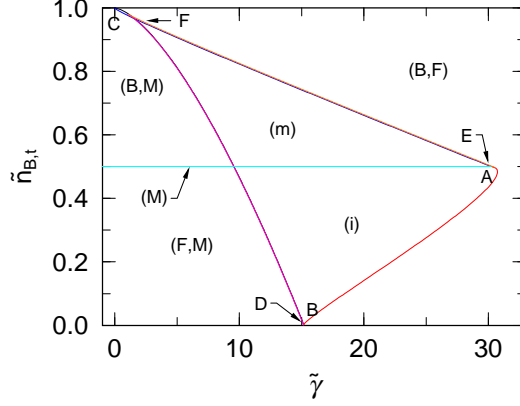


FIG. 11: (Color online) The $T = 0$ phase diagram of interacting BF mixtures with the same atom masses in the $\tilde{\gamma}$ - $\tilde{n}_{B,t}$ plane for $\tilde{\alpha} = -70$, where the phase (i) and (m) are coexisting phases of (B, F) , (F, M) and (B, F) , (B, M) as explained in the legend in Fig. 10(d).

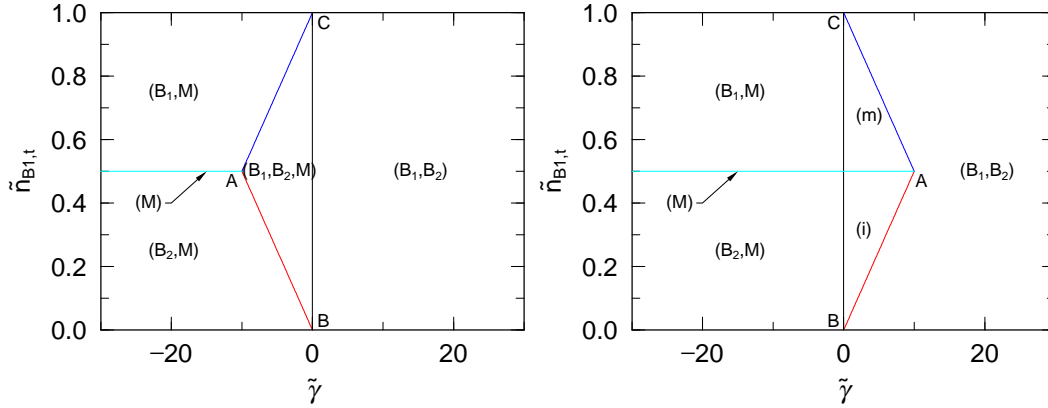


FIG. 12: (Color online) The $T = 0$ phase diagram of interacting BB mixtures with the same atom masses in the $\tilde{\gamma}$ - $\tilde{n}_{B1,t}$ plane for $\tilde{\alpha} = 20$ [(a), left] and $\tilde{\alpha} = -20$ [(b), right], where the phases (i) and (m) are coexisting phases of $(B1, B2)$, $(B2, M)$ and $(B1, B2)$, $(B1, M)$.

the phase structure in $\tilde{\alpha} > 0$ is just PS1. When $\tilde{\alpha} < 0$, Eq. (52) shows that point A moves across the boundary BC and locates to the right of it; the mixed phase disappears and new phases occur with coexisting locally stable equilibrium states [Fig. 12(b)]. That means that the phase structure is PS3 for $\tilde{\alpha} < 0$. As a result, we find $\tilde{\alpha}_{c1}^{(BB)} = \tilde{\alpha}_{c2}^{(BB)} = 0$ and no PS2 phase structures exist in the interacting BB mixtures.

In the case of interacting FF mixtures, the critical values $\tilde{\alpha}_{c1}^{(FF)}$ and $\tilde{\alpha}_{c2}^{(FF)}$ become

$$\tilde{\alpha}_{c1}^{(FF)} = -\frac{2}{3} \left(\tilde{m}_{F1}^{-3/4} + \tilde{m}_{F1}^{-3/4} \right)^{4/3}, \quad (53)$$

$$\tilde{\alpha}_{c2}^{(FF)} = -2^{1/3} \left(\frac{3\pi^2}{\sqrt{2}} \right)^{2/3} \frac{1}{\tilde{m}_{F1}\tilde{m}_{F2}}, \quad (54)$$

which become $\tilde{\alpha}_{c1}^{(FF)} \sim -25.5$ and $\tilde{\alpha}_{c2}^{(FF)} \sim -38.2$ in the case of $\tilde{m}_{F1} = \tilde{m}_{F2} = 1/2$.

In Fig. 13, we show the $T = 0$ phase diagrams for interacting FF mixtures with $\tilde{m}_{F1} = \tilde{m}_{F2} = 1/2$. The change of the phase structure is essentially similar to that in the interacting BF mixtures. In the PS1 structure [Fig. 13(a)], the phase structures are obtained by deformation from the noninteracting ones. The substructures with the coexisting states appear in the mixed phase in the PS2 structure [Fig. 13(b)]. The end point A in Fig. 13(a) and 13(b) crosses the boundary BC between the mixed and dissociated phases and new phases appear in the PS3 structure with the coexisting equilibrium states,

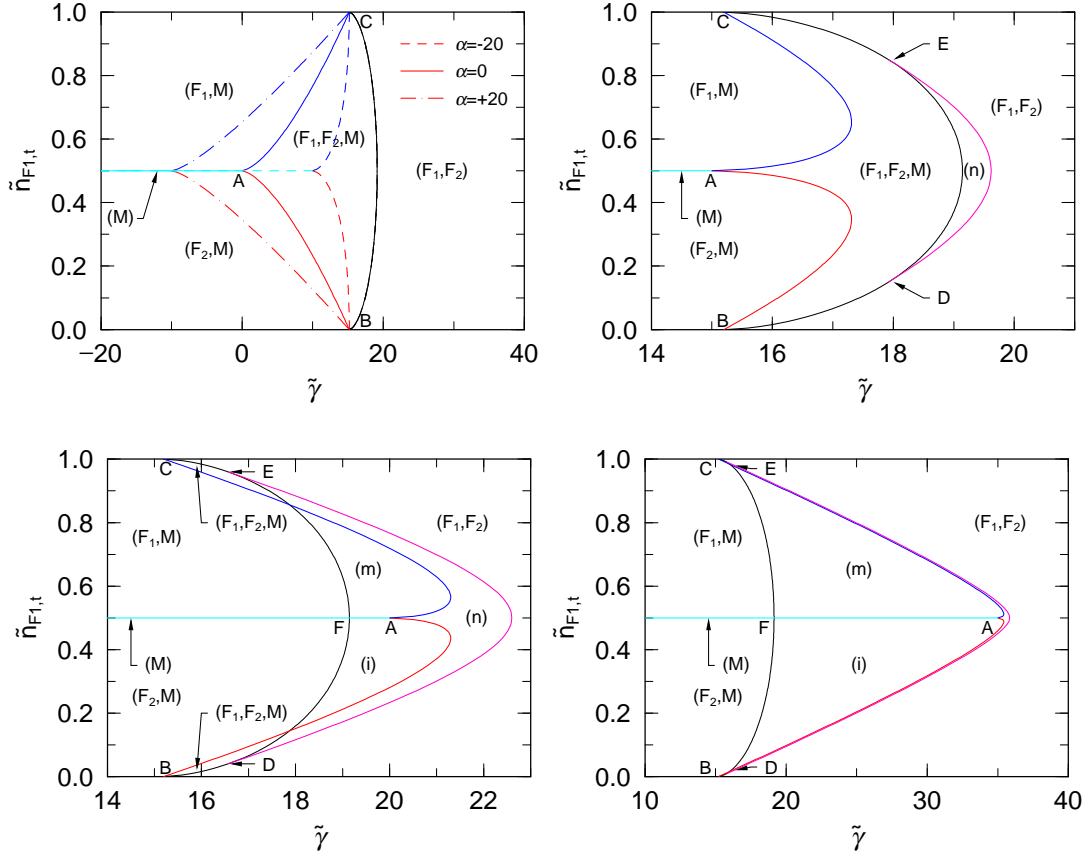


FIG. 13: (Color online) The $T = 0$ phase diagram of interacting FF mixtures with the same atom masses in the $\tilde{\gamma}$ - $\tilde{n}_{F1,t}$ plane for $\tilde{\alpha} = 20, 0, -20$ [(a), top left], -30 [(b), top right], -40 [(c), bottom left], and -70 [(d), bottom right], where the phases (i), (m), and (n) are coexisting phases of $(F1, F2)$, $(F2, M)$; $(F1, F2)$, $(F1, M)$; and $(F1, F2)$, $(F1, F2, M)$.

which have complex substructures [Fig. 13(c)]; the structure becomes again simple for large negative values of $\tilde{\alpha}$ [Fig. 13(d)].

VI. SUMMARY AND OUTLOOK

We have developed a quasichemical equilibrium theory for the molecular formation or dissociation processes in BF, FF, and BB mixtures of ultracold atomic gases and discussed atom-molecule equilibrium in these mixture.

The law of mass actions has also been examined for the mixtures; it is satisfied well at high T . We have shown that the quantum-statistical effects of the atoms and molecules, which become more effective in ultracold temperature, give deviations from the law (law of quantum mass action). The quantum-statistical effects are shown to give different deviations for bosons and fermions, and, in BF mixtures, both contributions have a tendency to cancel out at high T .

We have also discussed the effects of the interparticle interactions in the mixture within the mean-field approximation at $T = 0$ and evaluated the shifts of the $T = 0$ phase structures of atom-molecule equilibrium in the mixtures. Especially, in the case of large repulsive interactions between atoms and molecules, the phase structures have been shown to change qualitatively with the occurrence of coexisting local-equilibrium states. We have given the conditions for the coupling constants with which the phase-structure changes occur. The atom-molecule equilibrium in interacting mixtures can be calculated also at finite temperatures within the present framework, and the results are planned to be published in another paper.

The other correlation effects beyond the mean-field approximations should also be important—for example, in the BCS-BEC crossover problem. Combining the method of the Beth-Uhlenbeck approach[51, 52] with the present quasichemical equilibrium theory, we should discuss the correlation effects and the crossover problem from a less model-independent point of view. A study along these lines is now ongoing and will be presented in the near future.

The authors thank T. Suzuki and T. Takayama for many useful discussions.

APPENDIX A: ASYMPTOTIC BEHAVIORS OF BOSE OR FERMI FUNCTIONS

In this appendix, we derive some formulas of the asymptotic behaviors of the Bose and Fermi functions (6) and (7) at $\nu \sim 0$ and $\nu \sim \pm\infty$.

Before we discuss the asymptotic behavior, we prove the relation between B_A and F_A :

$$F_A(\nu) = B_A(\nu) - 2^{1-A}B_A(2\nu). \quad (\text{A1})$$

This formula is obtained by integrating both sides of the equation

$$\frac{x^{A-1}}{e^{x+\nu} + 1} = \frac{x^{A-1}}{e^{x+\nu} - 1} - \frac{2x^{A-a}}{e^{2x+2\nu} - 1}. \quad (\text{A2})$$

Let us go to the asymptotic behavior of the functions $B_A(\nu)$ and $F_A(\nu)$ at $\nu \sim \infty$. Using the expansion of the integrand of B_A ,

$$\frac{x^{A-1}}{e^{x+\nu} - 1} = \sum_{k=1}^{\infty} x^{A-1} e^{-k(x+\nu)}, \quad (\text{A3})$$

we obtain

$$B_A(\nu) = \sum_{k=1}^{\infty} \frac{e^{-k\nu}}{\Gamma(A)} \int_0^{\infty} x^{A-1} e^{-kx} dx = \sum_{k=1}^{\infty} \frac{e^{-k\nu}}{k^A}, \quad (\text{A4})$$

where we have used the formula of the gamma function:

$$\Gamma(A) = \int_0^{\infty} z^{A-1} e^{-z} dz. \quad (\text{A5})$$

Substituting (A4) into (A1), an expansion formula for $F_A(\nu)$ can be obtained:

$$F_A(\nu) = \sum_{k=1}^{\infty} (-1)^{k-1} \frac{e^{-k\nu}}{k^A}. \quad (\text{A6})$$

Taking the first terms in Eqs. (A4) and (A6), we obtain the asymptotic behaviors of $B_A(\nu)$ and $F_A(\nu)$ at $\nu \sim \infty$:

$$B_A(\nu) \sim F_A(\nu) \sim e^{-\nu}. \quad (\text{A7})$$

We turn to the asymptotic behavior of $B_A(\nu)$ around $\nu = 0$. When $0 < \alpha < 1$, the point $\nu = 0$ becomes an irregular singular point, so that only the asymptotic expansion is obtained for B_A . For this purpose, we consider the Hankel-type complex integral

$$I = \frac{1}{\Gamma(A)} \int_{(\infty; -\nu+)} \frac{z^{A-1} dz}{e^{z+\nu} - 1}. \quad (\text{A8})$$

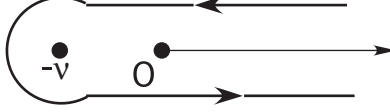


FIG. 14: Hankel-type integral path in the complex-number plane.

The integration path $(\infty; -\nu+)$ and the cut line on the positive real axis are shown in Fig. 14. The phase branches of z^{A-1} are fixed at x^{A-1} or $e^{2\pi Ai}x^{A-1}$ on the upper or lower parts of the cut line. The integrand function has a pole at $z = -\nu$:

$$\frac{z^{A-1}}{e^{z+\nu} - 1} \sim \frac{(-\nu)^{A-1}}{z + \nu}. \quad (\text{A9})$$

The integration path does not pass the singular point $z = -\nu$, so that we can evaluate the integral using the expansion (A2):

$$I = \sum_{k=1}^{\infty} \frac{e^{-k\nu}}{\Gamma(A)} \int_{(\infty; 0+)} z^{A-1} e^{-kz} dz = \sum_{k=1}^{\infty} \frac{e^{-k\nu}}{k^A} (e^{2\pi Ai} - 1), \quad (\text{A10})$$

where we have used the Hankel-integral representation of the gamma function.

On the other hand, we can deform the integration path and divide it into the path $C_{-\nu}$ circulating around the singular point $z = -\nu$ and the Hankel-type path $(\infty; 0+)$ around the origin O :

$$I = \frac{1}{\Gamma(A)} \int_{(\infty; -\nu+)} \frac{z^{A-1} dz}{e^{z+\nu} - 1} = \frac{1}{\Gamma(A)} \left[\oint_{C_{-\nu}} + \int_{(\infty; 0+)} \right] \frac{z^{A-1} dz}{e^{z+\nu} - 1}. \quad (\text{A11})$$

The integral on $C_{-\nu}$ is evaluated by the theorem of residue, and that on $(\infty; 0+)$ can be attributed to the real integral:

$$\frac{1}{\Gamma(A)} \oint_{C_{-\nu}} \frac{z^{A-1} dz}{e^{z+\nu} - 1} = \frac{2\pi i}{\Gamma(A)} (-\nu)^{A-1}, \quad (\text{A12})$$

$$\frac{1}{\Gamma(A)} \int_{(\infty; 0+)} \frac{z^{A-1} dz}{e^{z+\nu} - 1} = \frac{e^{2\pi i A} - 1}{\Gamma(A)} \int_0^{\infty} \frac{x^{A-1} dx}{e^{x+\nu} - 1} = (e^{2\pi i A} - 1) B_A(\nu). \quad (\text{A13})$$

Combining Eqs. (A10), (A12), and (A13), we obtain the asymptotic expansion of $B_A(\nu)$:

$$B_A(\nu) = \frac{\pi}{\sin \pi A} \frac{\nu^{A-1}}{\Gamma(A)} + \sum_{k=1}^{\infty} \frac{e^{-k\nu}}{k^A}. \quad (\text{A14})$$

Using the expansion of the series part in (A14),

$$\sum_{k=1}^{\infty} \frac{e^{-k\nu}}{k^A} = \sum_{k=1}^{\infty} \frac{1}{k^A} \sum_{n=0}^{\infty} \frac{(-k\nu)^n}{n!} = \sum_{n=0}^{\infty} \frac{(-\nu)^n}{n!} \sum_{k=1}^{\infty} \frac{1}{k^{A-n}} = \sum_{n=0}^{\infty} (-1)^n \zeta(A-n) \frac{\nu^n}{n!}, \quad (\text{A15})$$

we obtain the power expansion formula by Opechowski[53, 54]:

$$B_A(\nu) = \frac{\pi}{\sin \pi A} \frac{\nu^{A-1}}{\Gamma(A)} + \sum_{n=0}^{\infty} (-1)^n \zeta(A-n) \frac{\nu^n}{n!}. \quad (\text{A16})$$

Taking the leading term of the Opechowski formula, we obtain the asymptotic behavior of $B_A(\nu)$ around $\nu = 0$:

$$B_A(\nu) \sim \begin{cases} \zeta(A) & (A > 1), \\ -\ln \nu & (A = 1), \\ \frac{\pi}{\sin \pi A} \frac{\nu^{A-1}}{\Gamma(A)} + \zeta(A) & (0 < A < 1). \end{cases} \quad (\text{A17})$$

Using Eq. (A1), the asymptotic formula of $F_A(\nu)$ around $\nu = 0$ becomes

$$F_A(\nu) \sim (1 - 2^{1-A})\zeta(A). \quad (\text{A18})$$

It should be noted that the residue term in $B_A(\nu)$ is canceled out in (A18); this is consistent with the fact that no such singular terms exist in $F_A(\nu)$ originally.

The asymptotic formula of $F_A(\nu)$ at $\nu \sim -\infty$ is obtained by the Sommerfeld expansion formula[54, 55]

$$\int_0^{\infty} \frac{\phi'(u)du}{e^{u-\alpha} + 1} \sim \phi(\alpha) + \sum_{n=1}^{\infty} 2F_{2n}(0)\phi^{(2n)}(\alpha), \quad (\text{A19})$$

where $\phi(u)$ is a ∞ -differentiable function and the coefficients $F_{2n}(0)$, the Fermi function at $\nu = 0$, are represented by the Bernoulli numbers B_n :

$$2F_{2n}(0) = \frac{(1 - 2^{1-2n})(2\pi)^{2n}}{(2n)!} B_n. \quad (\text{A20})$$

Using Eq. (A19), the asymptotic formula of $F_A(\nu)$ at $\nu \sim -\infty$ is obtained by

$$F_A(\nu) \sim \frac{(-\nu)^A}{\Gamma(A+1)}. \quad (\text{A21})$$

APPENDIX B: DERIVATIONS OF $T = 0$ PHASE DIAGRAMS IN BF AND FF MIXTURES

1. Noninteracting BF mixture

Let us consider the mixed phase of the BF mixture of atom masses $\tilde{m}_{B,F}$, which corresponds to the central region in the phase diagram (Fig. 1). The equilibrium condition (9) becomes

$$0 + \left(\frac{3\pi^2}{\sqrt{2}}\right)^{2/3} \frac{1}{\tilde{m}_F} (\tilde{n}_F)^{2/3} - \left(\frac{3\pi^2}{\sqrt{2}}\right)^{2/3} (\tilde{n}_M)^{2/3} = \Delta \tilde{E}_M, \quad (\text{B1})$$

where we have used $\mu_B = 0$ (BEC state) and the Fermi energy formula (16) for F and M with $\tilde{m}_M \sim 1$.

The boundaries AB , BC , and CA in Fig. 1 are obtained by setting $\tilde{n}_B = 0$, $\tilde{n}_M = 0$, and $\tilde{n}_F = 0$, respectively:

$$AB : \quad \Delta\tilde{E}_M = \frac{1}{2\tilde{m}_F}[6\pi^2(1 - 2\tilde{n}_{B,t})]^{2/3} - \frac{1}{2}[6\pi^2\tilde{n}_{B,t}]^{2/3}, \quad (B2)$$

$$BC : \quad \Delta\tilde{E}_M = \frac{1}{2\tilde{m}_F}[6\pi^2\tilde{n}_{F,t}]^{2/3}, \quad (B3)$$

$$CA : \quad \Delta\tilde{E}_M = -\frac{1}{2}[6\pi^2\tilde{n}_{F,t}]^{2/3}. \quad (B4)$$

and the end points of the boundaries, A , B , and C , are obtained from (B4) with $\tilde{n}_{F,t} = 1/2$, (B3) with $\tilde{n}_{F,t} = 1$, and (B3) with $\tilde{n}_{F,t} = 0$:

$$A : \quad \Delta\tilde{E}_M = -\frac{(3\pi^2)^{2/3}}{2} \sim -4.8, \quad (B5)$$

$$B : \quad \Delta\tilde{E}_M = \frac{1}{2\tilde{m}_F}(6\pi^2)^{2/3} \sim \frac{7.6}{\tilde{m}_F}, \quad (B6)$$

$$C : \quad \Delta\tilde{E}_M = 0. \quad (B7)$$

The boundaries and end points in Fig. 1 are obtained from the above formulas for $\tilde{m}_F = 1/2$.

2. Noninteracting FF mixture

In the case of the phase diagram of the FF mixture (Fig. 3) with masses \tilde{m}_{F1} and \tilde{m}_{F2} , the equilibrium condition (9) in the mixed phase becomes

$$\left(\frac{3\pi^2}{\sqrt{2}}\right)^{2/3} \frac{1}{\tilde{m}_{F1}}(\tilde{n}_{F1})^{2/3} + \left(\frac{3\pi^2}{\sqrt{2}}\right)^{2/3} \frac{1}{\tilde{m}_{F2}}(\tilde{n}_{F2})^{2/3} = \Delta\tilde{E}_M, \quad (B8)$$

where we have used $\mu_M = 0$ (BEC state) and the Fermi energy formula (16) for $F1$ and $F2$.

The boundaries AB , BC , and CA in Fig. 3 are obtained by setting $\tilde{n}_{F2} = 0$, $\tilde{n}_M = 0$, and $\tilde{n}_{F1} = 0$, respectively:

$$AB : \quad \Delta\tilde{E}_M = \frac{1}{2\tilde{m}_{F1}}[6\pi^2(1 - 2\tilde{n}_{F1,t})]^{2/3}, \quad (B9)$$

$$BC : \quad \Delta\tilde{E}_M = \frac{1}{2\tilde{m}_{F1}}[6\pi^2\tilde{n}_{F1,t}]^{2/3} + \frac{1}{2\tilde{m}_{F2}}[6\pi^2\tilde{n}_{F2,t}]^{2/3}, \quad (B10)$$

$$CA : \quad \Delta\tilde{E}_M = \frac{1}{2\tilde{m}_{F2}}[6\pi^2(2\tilde{n}_{F1,t} - 1)]^{2/3}, \quad (B11)$$

and the points A , B and C are obtained from (B9) with $\tilde{n}_{F1,t} = 1/2$, (B9) with $\tilde{n}_{F1,t} = 0$, and (B11) with $\tilde{n}_{F1,t} = 1$:

$$A : \quad \Delta \tilde{E}_M = 0, \quad (\text{B12})$$

$$B : \quad \Delta \tilde{E}_M = \frac{1}{2\tilde{m}_{F1}}(6\pi^2)^{2/3} \sim \frac{7.6}{\tilde{m}_{F2}}, \quad (\text{B13})$$

$$C : \quad \Delta \tilde{E}_M = \frac{1}{2\tilde{m}_{F2}}(6\pi^2)^{2/3} \sim \frac{7.6}{\tilde{m}_{F1}}. \quad (\text{B14})$$

The boundaries and end points in Fig. 3 are obtained from the above formulas with $\tilde{m}_{F1} = \tilde{m}_{F2} = 1/2$.

3. Interacting BF mixture

The $T = 0$ phase diagram of the interacting BF mixture with masses $\tilde{m}_{B,F}$ is obtained by the equilibrium condition (48) for $T = 0$:

$$0 + \left(\frac{3\pi^2}{\sqrt{2}}\right)^{2/3} \frac{1}{\tilde{m}_F}(\tilde{n}_F)^{2/3} - \left(\frac{3\pi^2}{\sqrt{2}}\right)^{2/3} (\tilde{n}_M)^{2/3} = \tilde{\alpha}\tilde{n}_M + \tilde{\gamma}. \quad (\text{B15})$$

In the case of $\tilde{\alpha} > \tilde{\alpha}_{c1}^{(BF)}$, the boundaries and end points of the phases can be obtained in the same manner as those in noninteracting cases.

The results are

$$AB : \quad \tilde{\gamma} = \left(\frac{3\pi^2}{\sqrt{2}}\right)^{2/3} \left[\frac{1}{\tilde{m}_F}(\tilde{n}_{F,t} - \tilde{n}_{B,t})^{2/3} - \tilde{n}_{B,t}^{2/3} \right] - \tilde{\alpha}\tilde{n}_{B,t}, \quad (\text{B16})$$

$$BC : \quad \tilde{\gamma} = \left(\frac{3\pi^2}{\sqrt{2}}\right)^{2/3} \frac{1}{\tilde{m}_F} \tilde{n}_{F,t}^{2/3}, \quad (\text{B17})$$

$$CA : \quad \tilde{\gamma} = - \left(\frac{3\pi^2}{\sqrt{2}}\right)^{2/3} \tilde{n}_{F,t}^{2/3} - \tilde{\alpha}\tilde{n}_{F,t}, \quad (\text{B18})$$

for the phase boundaries ($\tilde{n}_{B,t} + \tilde{n}_{F,t} = 1$), and

$$A : \quad \tilde{\gamma} = - \left(\frac{3\pi^2}{2\sqrt{2}}\right)^{2/3} - \frac{\tilde{\alpha}}{2} \sim -4.78 - \frac{\tilde{\alpha}}{2}, \quad (\text{B19})$$

$$B : \quad \tilde{\gamma} = \frac{1}{\tilde{m}_F} \left(\frac{3\pi^2}{\sqrt{2}}\right)^{2/3} \sim \frac{7.6}{\tilde{m}_F}, \quad (\text{B20})$$

$$C : \quad \tilde{\gamma} = 0. \quad (\text{B21})$$

The boundaries and end points in Fig. 7 are obtained from the above formulas with $\tilde{m}_F = \tilde{m}_B = 1/2$.

4. Interacting BB mixture

The $T = 0$ phase diagram of the interacting BB mixture with masses $\tilde{m}_{B1,B2}$ is obtained by the equilibrium condition (48).

At $T = 0$, all chemical potentials appearing in (48), which are bosonic, can take two alternative possibilities: $\tilde{\mu}'_k = 0$ with $\tilde{n}_k \neq 0$ (BEC) or $\tilde{\mu}'_k < 0$ with $\tilde{n}_k = 0$ ($k = B1, B2, M$).

In the mixed phase, the BEC conditions $\tilde{\mu}'_{B1} = \tilde{\mu}'_{B2} = \tilde{\mu}'_M = 0$ give $\tilde{\alpha}\tilde{n}_M + \tilde{\gamma} = 0$; the boundaries, AB , BC , and CA , are obtained by substituting $\tilde{n}_{B2} = 0$, $\tilde{n}_M = 0$, and $\tilde{n}_{B1} = 0$, respectively:

$$AB : \quad \tilde{\gamma} = -\tilde{\alpha}\tilde{n}_{B1,t}, \quad (\text{B22})$$

$$BC : \quad \tilde{\gamma} = 0, \quad (\text{B23})$$

$$CA : \quad \tilde{\gamma} = -\tilde{\alpha}(1 - \tilde{n}_{B1,t}), \quad (\text{B24})$$

where we have used the constraints $\tilde{n}_{B1} + \tilde{n}_M = \tilde{n}_{B1,t}$ and $\tilde{n}_{B2} + \tilde{n}_M = \tilde{n}_{B2,t}$. The end points are obtained by

$$A : \quad \tilde{\gamma} = -\frac{\tilde{\alpha}}{2}, \quad (\text{B25})$$

$$B : \quad \tilde{\gamma} = 0, \quad (\text{B26})$$

$$C : \quad \tilde{\gamma} = 0. \quad (\text{B27})$$

It should be noted that the boundaries and the end points are independent of the atom masses $\tilde{m}_{B1,B2}$.

5. Interacting FF mixture

The $T = 0$ phase diagram of the interacting FF mixture with masses $\tilde{m}_{B,F}$ is obtained by the equilibrium condition (48). for $T = 0$:

$$\left(\frac{3\pi^2}{\sqrt{2}}\right)^{2/3} \frac{1}{\tilde{m}_{F1}}(\tilde{n}_{F1})^{2/3} + \left(\frac{3\pi^2}{\sqrt{2}}\right)^{2/3} \frac{1}{\tilde{m}_{F2}}(\tilde{n}_{F2})^{2/3} = \tilde{\alpha}\tilde{n}_M + \tilde{\gamma}. \quad (\text{B28})$$

In the case of $\tilde{\alpha} > \tilde{\alpha}_{c1}^{(FF)}$, the boundaries and end points of the phases can be obtained in the same manner as those in noninteracting cases.

The results are

$$AB : \quad \tilde{\gamma} = \frac{1}{2\tilde{m}_{F1}} [6\pi^2(1 - 2\tilde{n}_{F1,t})]^{2/3} - \tilde{\alpha}\tilde{n}_{F1,t}, \quad (\text{B29})$$

$$BC : \quad \tilde{\gamma} = \frac{1}{2\tilde{m}_{F1}} [6\pi^2\tilde{n}_{F1,t}]^{2/3} + \frac{1}{2\tilde{m}_{F2}} [6\pi^2\tilde{n}_{F2,t}]^{2/3}, \quad (\text{B30})$$

$$CA : \quad \tilde{\gamma} = \frac{1}{2\tilde{m}_{F2}} [6\pi^2(2\tilde{n}_{F1,t} - 1)]^{2/3} + \tilde{\alpha}(\tilde{n}_{F1,t} - 1), \quad (\text{B31})$$

for the phase boundaries ($\tilde{n}_{B,t} + \tilde{n}_{F,t} = 1$), and

$$A : \quad \tilde{\gamma} = -\frac{\tilde{\alpha}}{2}, \quad (\text{B32})$$

$$B : \quad \tilde{\gamma} = \frac{1}{2\tilde{m}_{F1}} (6\pi^2)^{2/3} \sim \frac{7.6}{\tilde{m}_{F2}}, \quad (\text{B33})$$

$$C : \quad \tilde{\gamma} = \frac{1}{2\tilde{m}_{F2}} (6\pi^2)^{2/3} \sim \frac{7.6}{\tilde{m}_{F1}}. \quad (\text{B34})$$

The boundaries and end points in Fig. 11 are obtained from the above formulas with $\tilde{m}_{F1} = \tilde{m}_{F2} = 1/2$.

-
- [1] E.A. Cornell and C.E. Wieman, Rev. Mod. Phys. **74**, 875 (2002);
W. Ketterle, Rev. Mod. Phys. **74**, 1131 (2002).
 - [2] F. Dalfovo, et al., Rev. Mod. Phys. **71**, 463 (1999).
 - [3] C. J. Pethik and H. Smith, *Bose-Einstein Condensation in Dilute Gases*, (Cambridge University Press, Cambridge, 2002).
 - [4] L. Pitaevskii and S. Stringari, *Bose-Einstein Condensation*, (Clarendon Press, Oxford, 2003)
 - [5] C. A. Regal, C. Ticknor, J. L. Bohn, and D. S. Jin, Nature **424**, 47 (2003).
 - [6] J. Cubizolles, T. Bourdel, S. J. J. M. F. Kokkelmans, G.V. Shlyapnikov, C. Salomon, Phys. Rev. Lett. **91**, 240401 (2003).
 - [7] R. Wynar, R. S. Freeland, D. J. Han, et.al., SCIENCE **287** (2000) 1016.
 - [8] S. Jochim, M. Bartenstein, A. Altmeyer, et.al., Phys. Rev. Lett. **91**, 240402 (2003).
 - [9] J. Herbig, T. Kraemer, M. Mark, et.al., Science **301**, 1510 (2003).
 - [10] M. Greiner, C. A. Regal, and D. S. Jin, Nature **426**, 537 (2003).
 - [11] M. N. Zwierlein, C. A. Stan, C. H. Schunck, et.al., Phys. Rev. Lett. **91**, 250401 (2003).
 - [12] M. R. Schafroth, J. M. Blatt, and S. T. Butler, Helv. Phys. Acta. **30**, 93 (1957); J. M. Blatt, *Theory of Superconductivity* (Academic Press, London, 1964).

- [13] A. J. Leggett, *Diatomic Molecules and Cooper Pairs*, in *Modern Trends in the Theory of Condensed Matter*, edited by A. Pekalski and R. Przystawa, (Springer-Verlag, Berlin, 1980).
- [14] P. Nozières and S. Schmidt-Rink, J. Low Temp. Phys. **59**, 195 (1985).
- [15] M. Randeria, *Crossover from BCS Theory to BEC in Bose-Einstein Condensation* eds. A. Griffin et.al. (Cambridge Univ., Cambridge, 1996).
- [16] M. Schmidt, G. Röpke, and H. Schulz, Ann. Phys. **202**, 57 (1990).
- [17] H. Stein, A. Schnell, T. Alm and G. Röpke, Z. Phys. **A351**, 295 (1995); G. Röpke, Z. Phys. **B99**, 83 (1996).
- [18] C. A. Regal, M. Greiner, and D. S. Jin, Phys. Rev. Lett. **92**, 040403 (2004).
- [19] M. Bartenstein, A. Altmeyer, S. Riedl, et.al., Phys. Rev. Lett. **92**, 120401 (2004).
- [20] M. N. Zwierlein, C. A. Stan, C. H. Schunck, et.al., Phys. Rev. Lett. **92**, 120403 (2004).
- [21] Y. Ohashi and A. Griffin, Phys. Rev. Lett. **89**, 130402 (2002); Phys. Rev. **A67**, 033603, 063612 (2003).
- [22] G. M. Falco and H. T. C. Stoof, Phys. Rev. Lett. **92**, 130401 (2004).
- [23] Q. Chen, J. Stajic, S. Tan, and K. Levin, Phys. Report **412**, 1 (2005).
- [24] C. Chin and R. Grimm, Phys. Rev. A **69**, 033612 (2004).
- [25] J. E. Williams, T. Nikuni, N. Nygaard, and C. W. Clark, J. Phys. B **37**, L351 (2004); J. E. Williams, N. Nygaard, and C. W. Clark, New J. Phys. **6**, 123 (2004); New J. Phys. **8**, 150 (2006); S. Watabe, T. Nikuni, N. Nygaard, J. E. Williams, and C. W. Clark, J. Phys. Soc. Jpn. **76**, 064003 (2007).
- [26] T. Rom, T. Best, O. Mandel, et.al., Phys. Rev. Lett. **93**, 073002 (2004).
- [27] G. Thalhammer, K. Winkler, F. Lang, et.al., Phys. Rev. Lett. **96**, 050402 (2006).
- [28] M. Köhl, H. Moritz, T. Stöferle, K. Gunter, T. Esslinger, Phys. Rev. Lett. **94**, 080403 (2005).
- [29] C. Ospelkaus, S. Ospelkaus, L. Humbert, et.al., Phys. Rev. Lett. **97**, 120402 (2006).
- [30] C. Ryu, X. Du, E. Yosilada, S. Wan, Q. Niu, and D. J. Heinzen, e-print cond-mat/0508201.
- [31] M. Greiner, O. Mandel, T. Esslinger, T. W. Hönsch, and I. Bloch, Nature (London) **415**, 39 (2002).
- [32] O. Mandel, M. Greiner, A. Widera, T. Rom, T. Hänsch, and I. Bloch, Nature (London) **425**, 937 (2003).
- [33] G. G. Batrouni, R. T. Scalettar, G. T. Zimanyi, Phys. Rev. Lett. **65**, 1765 (1990).
- [34] D. Jaksch, C. Bruder, J. I. Cirac, C. W. Gardiner, and P. Zoller, Phys. Rev. Lett. **81**, 3108

- (1998).
- [35] M. W. Jack and M. Yamashita, Phys. Rev. **A67**, 033605 (2003).
 - [36] G. Roati, E. de Mirandes, F. Ferlaino, H. Ott, G. Modugno, and M. Inguscio, Phys. Rev. Lett. **92**, 230402 (2004).
 - [37] Y. Fujiwara, A. Koga, and N. Kawakami, J. Phys. Soc. Japan **76**, 034716 (2007).
 - [38] T. Miyakawa and P. Meystre, Phys. Rev. **A74**, 043615 (2006).
 - [39] P. D. Drummond, K. V. Kheruntsyan, and H. He, Phys. Rev. Lett. **81**, 3055 (1998).
 - [40] J. Javanainen and M. Mackie, Phys. Rev. **A59**, R3186 (1999).
 - [41] E. Timmermans, P. Tommasini, R. Coté, M. Hussein, and A. Kerman, Phys. Rev. Lett. **83**, 2691 (1999).
 - [42] P. Atkins, J. De Paula, *Atkins' Physical Chemistry*, (8Rev Ed; Oxford University Press, New York, 2006)
 - [43] K. J. Laidler, *Chemical Kinetics*, (McGraw-Hill Inc., New York, 1965).
 - [44] H. Yabu, Y. Takayama, and T. Suzuki, Physica **B329-333**, 25 (2003).
 - [45] H. Yabu, Y. Takayama, T. Suzuki, and P. Schuck, Nucl. Phys. **A738**, 273 (2004).
 - [46] A. Storozhenko, P. Schuck, T. Suzuki, H. Yabu, and J. Dukelsky, Phys. rev. **A71**, 063617 (2005).
 - [47] M. A. Morales, N. Nygaard, J. E. Williams and C. W. Clark, New J. Phys. **7**, 87 (2005).
 - [48] K. Nawa, E. Nakano, and H. Yabu, Phys. Rev. **D74**, 034017 (2006).
 - [49] L. D. Landau, et.al., *Statistical Physics* (Course of Theoretical Physics, Vol. 5), translated by J. B. Sykes and M. J. Kearsley, (Butterworth-Heinemann, Oxford, 1984).
 - [50] K. Huang, *Statistical Mechanics*, (2nd ed., John Wiley & Sons, 1987).
 - [51] G. E. Beth and E. Uhlenbeck, Physica **4**, 915 (1937).
 - [52] M. Schmidt, G. Röpke and H. Schulz, Ann. Phys. **202**, 57 (1990).
 - [53] W. Opechowski, Physica **4**, 722 (1937).
 - [54] D. ter Haar, *Elements of Statistical Mechanics*, (Rinehart & Company, Inc., New York, 1956).
 - [55] A. Sommerfeld, Z. Phys. **47**, 1 (1928).